

Climate Change Impacts in the Middle East

2030, 2050, 2075

01

Storms & Coastal Issues

Sea level rise, cyclones, and extreme rainfall

02

Extreme Heat

Human heat stress, high-density altitude, infrastructure

03

Drought & Water Supply

Water supply, desertification, and dust

Supplemental

- 01 Climate Zones & Warming Scenarios
- 02 Storms & Coastal Issues: Heavy Precipitation, Sea Level Rise
- 03 Extreme Heat: Frequency of Black Flag Days & Higher Temperatures
- 04 Drought
- 07 Water Supply
- 10 Wind
- 10 Data Analysis Methods: Historical Data, Future Climate Projections, Metrics



Middle East: Storms & Coastal Issues

Extreme rainfall events and destructive flash flooding, which are already common, plus devastating cyclones are projected to increase and interact with sea level rise in coastal areas, exacerbating hazards.



Increased extreme rainfall and flash flooding will cause localized destruction in Yemen, southwestern Saudi Arabia, and western Oman, potentially exacerbating or causing cholera outbreaks and driving displacement.



Warming seas and moister air will make the Arabian peninsula more vulnerable to tropical cyclones and their impacts.



The Red Sea and Arabian Gulf are rising at an accelerated rate compared to global trends as winds and other local parameters interact with the small basin size to generate highly dynamic max and min sea levels.



Extreme sea levels are amplified in winter and have reached as high as 0.85m in the northern Gulf of Suez and 0.3-0.5m over the rest of the Red Sea.

Select Installations in the Middle East:

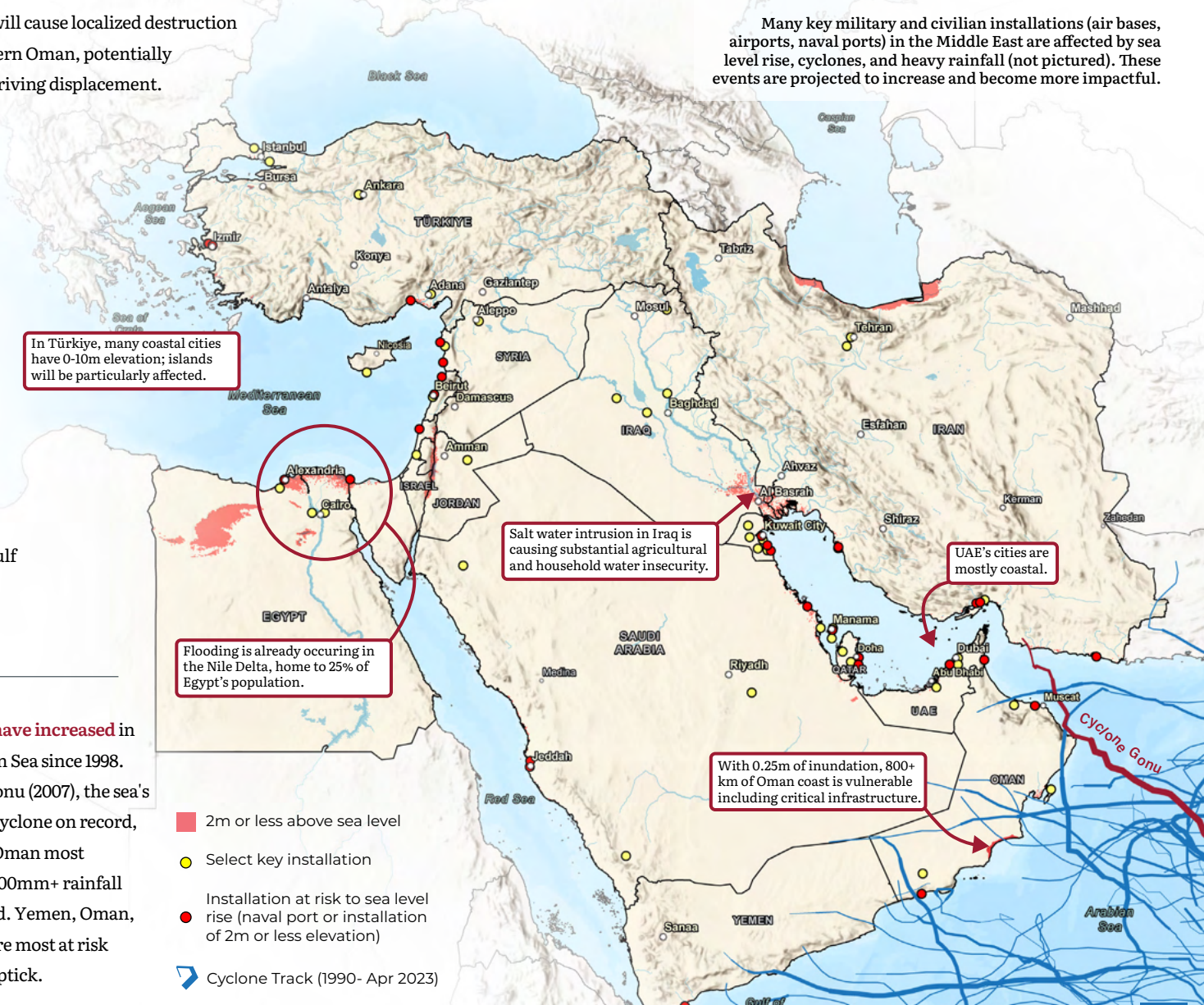
Many key military and civilian installations (air bases, airports, naval ports) in the Middle East are affected by sea level rise, cyclones, and heavy rainfall (not pictured). These events are projected to increase and become more impactful.

Recent Storm Impacts

Water-resistant soils, impervious surfaces, and sheetflow off slopes create hazardous conditions that cause flash floods.

- In 2009, 70 mm of rain in 3 hours in Jeddah, SA killed 113 people and destroyed 10K+ homes.
- A 30-minute extreme rain event at an Air Force Base in Khazor, Israel, (2020) flooded an underground F-16 hangar, and mechanics had to be rescued.

Cyclones have increased in the Arabian Sea since 1998. Cyclone Gonu (2007), the sea's strongest cyclone on record, impacted Oman most acutely—600mm+ rainfall and 50 dead. Yemen, Oman, and UAE are most at risk from the uptick.



By 2075, temperatures on average will increase approximately 4°C across the Middle East, increasing black flag days, hindering flight operations, and damaging infrastructure.



Dark-asphalt roads begin to **soften at 50°C**, which can happen at an air temperature of 20°C. Air temps approaching 50°C begin to impact other infrastructure. While 50°C days are rare they will occur with increasing frequency in the future.

Difference in Mean Frequency of Days above 32°C

Difference between historic (1990-2020) and 2075

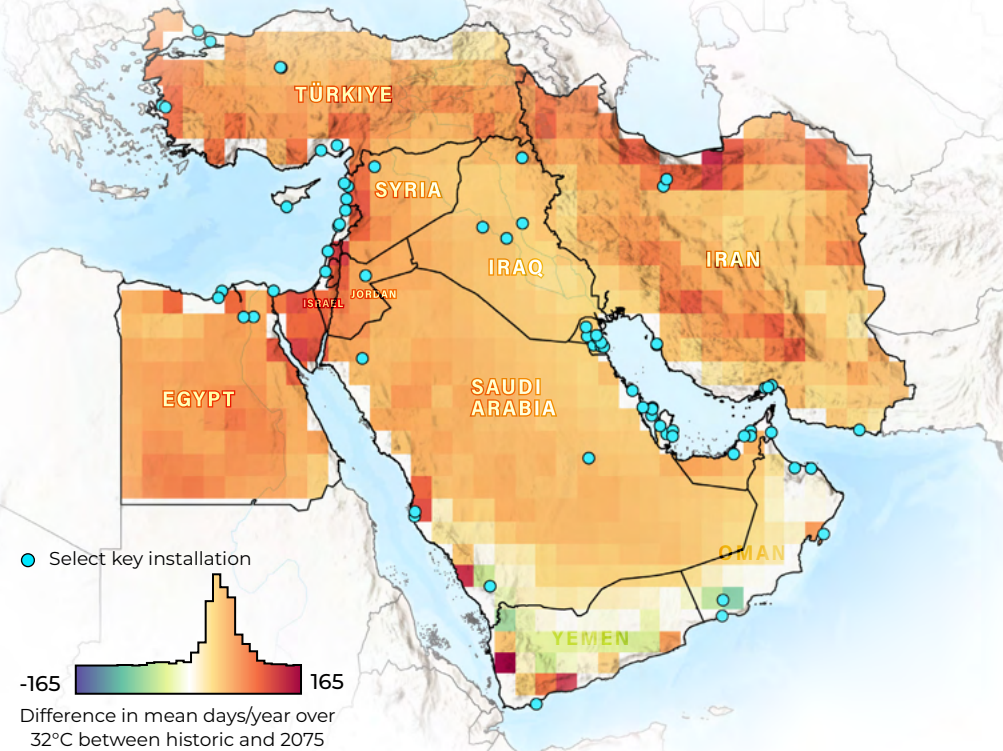
Temperatures in the arid, hot regions are already above 32°C (black flag days) nearly half the year. Under the extreme warming scenario, **48 more black flag days a year** are likely by 2075.



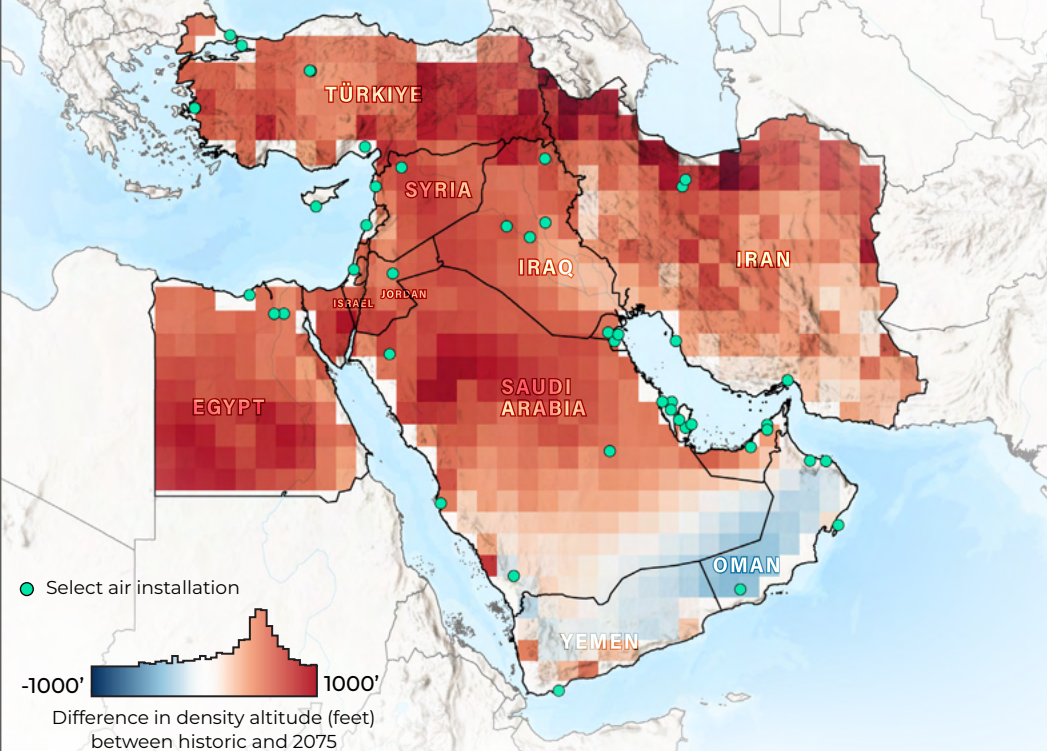
Density altitude increases due to extreme heat will **degrade aircraft performance**, with strongest effects in arid and high-altitude regions. Eastern Iran and western Saudi Arabia may need runway extensions as early as 2050. Helicopters and cargo aircraft will be most acutely affected.

Density Altitude Change in Summer

(June, July, August) from historic (1990-2020) to 2075 Density altitude will increase by up to 1000 feet across the Middle East except for coastal Yemen and Oman, where a decrease is projected, based on average daily temperatures.



Data: CMIP6



Current Extreme Heat Impacts

Runways and carrier flight decks reach temps up to 65°C in the Middle East and North Africa, reducing exertion abilities of ground control, contributing to malfunctions and corrosion of hardware, inducing weight-restriction days, and decreasing combat radius.

Most roads in the region fail before a **25- to 30-year lifespan** from current heat and flood conditions. In Saudi Arabia, substantial rutting of roads occurs within two to seven service years. Temperature increases will exacerbate conditions of roads not engineered for extreme heat.



Rainfall will decrease 30% in temperate and boreal climate zones including Türkiye, Iran, and parts of Iraq by 2075. Annual rainfall will be difficult to predict as variation will increase as time progresses.



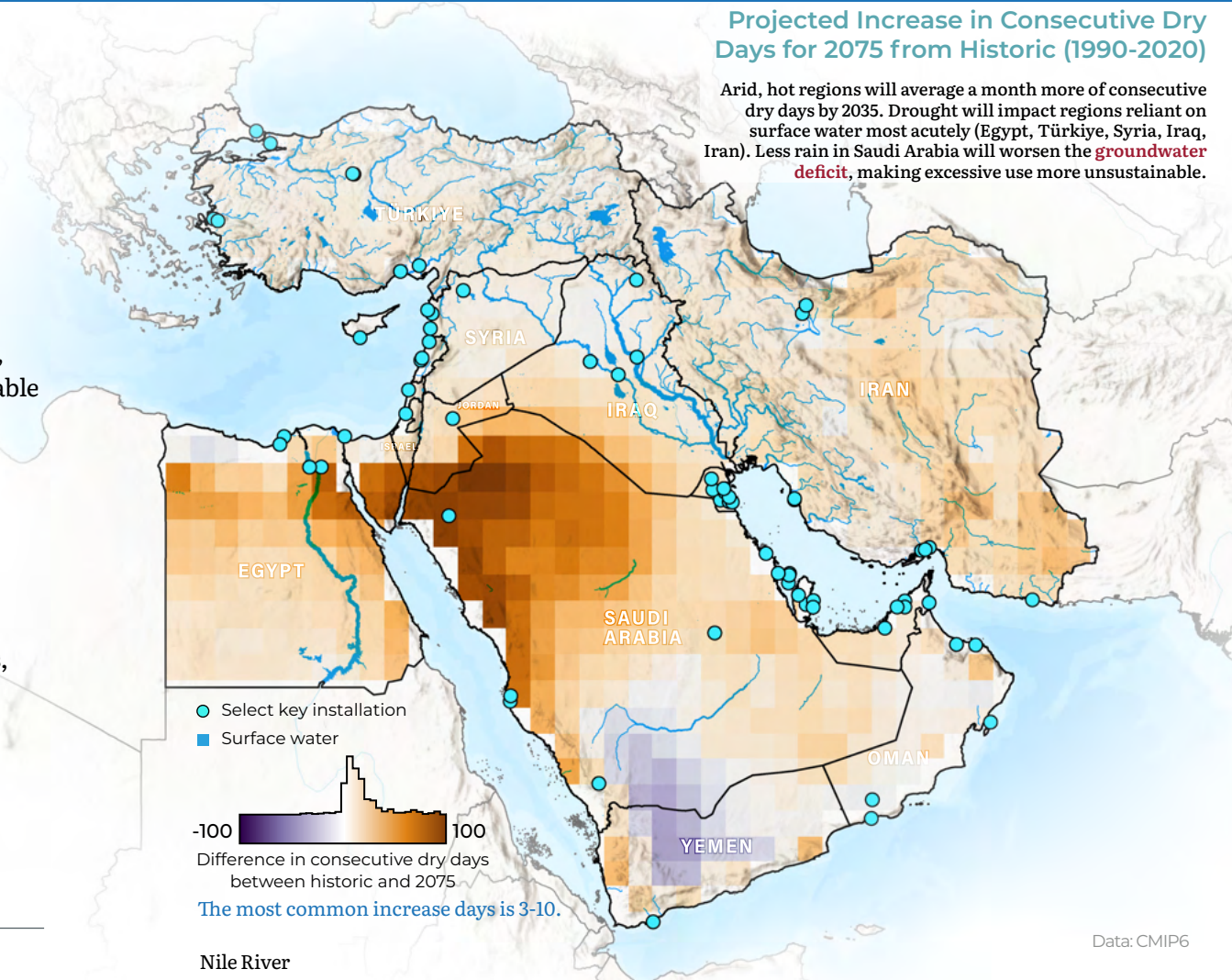
Persistent drought will damage rainfed crops, diminish irrigation capabilities, hinder sustainable agriculture in Türkiye, Egypt and the Levant region, and lower economic productivity.



Excess dust created by water extractions and drought increases destructive dust storms that can lower visibility, hinder flights, halt vehicles, penetrate weapon system mechanics, damage solar panels, and cause major respiratory issues like fungal or hantavirus infections.

Projected Increase in Consecutive Dry Days for 2075 from Historic (1990-2020)

Arid, hot regions will average a month more of consecutive dry days by 2035. Drought will impact regions reliant on surface water most acutely (Egypt, Türkiye, Syria, Iraq, Iran). Less rain in Saudi Arabia will worsen the **groundwater deficit**, making excessive use more unsustainable.



Data: CMIP6

Key Water Supply Issues

Tigris & Euphrates Rivers

- Dams in Türkiye, drought, and extraction are causing low flows into Syria and Iraq, resulting in saltwater intrusion from the Gulf into ground and surface water. This will exacerbate the already significant problem with household and agricultural water insecurity and pollution that is causing cholera outbreaks.
- Warming will decrease upstream snowmelt contributions, and drought will worsen the water security situation in the region.

Nile River

- The Nile Delta is experiencing **extreme sinking** caused by sediment-trapping upstream dams. Low river flows from drought and extraction in concert with rising sea level is causing of ground and surface water and further loss of land.
- Less rainfall and reduced flow from the planned Great Ethiopian Renaissance Dam will further jeopardize water supply for Egypt.

Sources:

- Abdulla, C. P., & Al-Subhi, A. M. (2021). Is the Red Sea Sea-Level Rising at a Faster Rate than the Global Average? An Analysis Based on Satellite Altimetry Data. *Remote Sensing*, 13(17), Article 17. <https://doi.org/10.3390/rs13173489>
- Al-Ansari, N., Ali, A. A., & Knutsson, S. (2014). Present Conditions and Future Challenges of Water Resources Problems in Iraq. *Journal of Water Resource and Protection*, 06(12), 1066–1098. <https://doi.org/10.4236/jwarp.2014.612102>
- Arias, P.A., et al., 20 21: Technical Summary. In *Climate Change 2021: The Physical Science Basis. Contribution of Working Group I to the Sixth Assessment Report of the Intergovernmental Panel on Climate Change* [Masson-Delmotte, V., P. Zhai, A. Pirani, S.L. Connors, C. Péan, S. Berger, N. Caud, Y. Chen, L. Goldfarb, M.I. Gomis, M. Huang, K. Leitzell, E. Lonnoy, J.B.R. Matthews, T.K. Maycock, T. Waterfield, O. Yelekçi, R. Yu, and B. Zhou (eds.)]. Cambridge University Press, Cambridge, United Kingdom and New York, NY, USA, pp. 33–144. doi:10.1017/9781009157896.002.
- Badughaish, A., et al. (2022). A review on the crumb rubber-modified asphalt in the Middle East. *Journal of Material Cycles and Waste Management*, 24(5), 1679–1692. <https://doi.org/10.1007/s10163-022-01455-0>
- CMIP Phase 6 (CMIP6). <https://esgf-node.llnl.gov/projects/cmip6/>
- Goodman, C. J., & Griswold, J. D. S. (2018). Climate Impacts on Density Altitude and Aviation Operations. *Journal of Applied Meteorology and Climatology*, 57(3), 517–523. <https://doi.org/10.1175/JAMC-D-17-0126.1>
- NASA/METI/AIST/Japan Spacesystems and U.S./Japan ASTER Science Team (2019). ASTER Global Digital Elevation Model V003. NASA EOSDIS Land Processes Distributed Active Archive Center. Accessed 2023-11-30 from <https://doi.org/10.5067/ASTER/ASTGTM.003>
- National Oceanic and Atmospheric Administration (NOAA). Knapp, K. R., et al. 2010: The International Best Track Archive for Climate Stewardship (IBTrACS): Unifying tropical cyclone best track data. *Bulletin of the American Meteorological Society*, 91, 363-376. doi:10.1175/2009BAMS2755.1 Knapp, K. R., H. J. Diamond, J. P. Kossin, M. C. Kruk, C. J. Schreck, 2018: International Best Track Archive for Climate Stewardship (IBTrACS) Project, Version 4. [indicate subset used]. NOAA National Centers for Environmental Information. doi:10.25921/82ty-9e16 [Accessed December 12, 2023].
- Oppenheimer, M., et al. (2019): Sea Level Rise and Implications for Low-Lying Islands, Coasts and Communities. In: *IPCC Special Report on the Ocean and Cryosphere in a Changing Climate* [H.-O. Pörtner, D.C. Roberts, V. Masson-Delmotte, P. Zhai, M. Tignor, E. Poloczanska, K. Mintenbeck, A. Alegría, M. Nicolai, A. Okem, J. Petzold, B. Rama, N.M. Weyer (eds.)]. Cambridge University Press, Cambridge, UK and New York, NY, USA, pp. 321-445. <https://doi.org/10.1017/9781009157964.006>.
- Vidya, P. J., et al. (2023). Intensification of Arabian Sea cyclone genesis potential and its association with Warm Arctic Cold Eurasia pattern. *Npj Climate and Atmospheric Science*, 6(1), Article 1. <https://doi.org/10.1038/s41612-023-00476-2>

Map Sources:

Esri, USGS, NOAA. Scale Not Given. “World Terrain Base”. May, 27, 2020. https://server.arcgisonline.com/ArcGIS/rest/services/World_Terrain_Base/MapServer. (May, 15, 2023).

Sources: Esri, Airbus DS, USGS, NGA, NASA, CGIAR, N Robinson, NCEAS, NLS, OS, NMA, Geodatastyrelsen, Rijkswaterstaat, GSA, Geoland, FEMA, Intermap, and the GIS user community. “World Hillshade”. February 10, 2022. https://services.arcgisonline.com/arcgis/rest/services/Elevation/World_Hillshade/MapServer. (May, 15, 2023).

Maps throughout this report were created using ArcGIS® software by Esri. ArcGIS® and ArcMap™ are the intellectual property of Esri and are used herein under license. Copyright © Esri. All rights reserved. For more information about Esri® software, please visit www.esri.com.

Supplemental Materials

Climate Zones & Warming Scenarios

Climate projections were analyzed using three different futures: 2035, 2050, and 2075. The historic period of comparison is 1990-2020. Two different warming scenarios were used for future projections. Shared Socioeconomic Pathway (SSP) 245 represents a conservative warming scenario, while SSP585 is a more extreme warming scenario. Generalized Koppen-Geiger climate zones were used to analyze projections by climate type (Figure 1).

Figure 1: Koppen-Geiger generalized climate zones



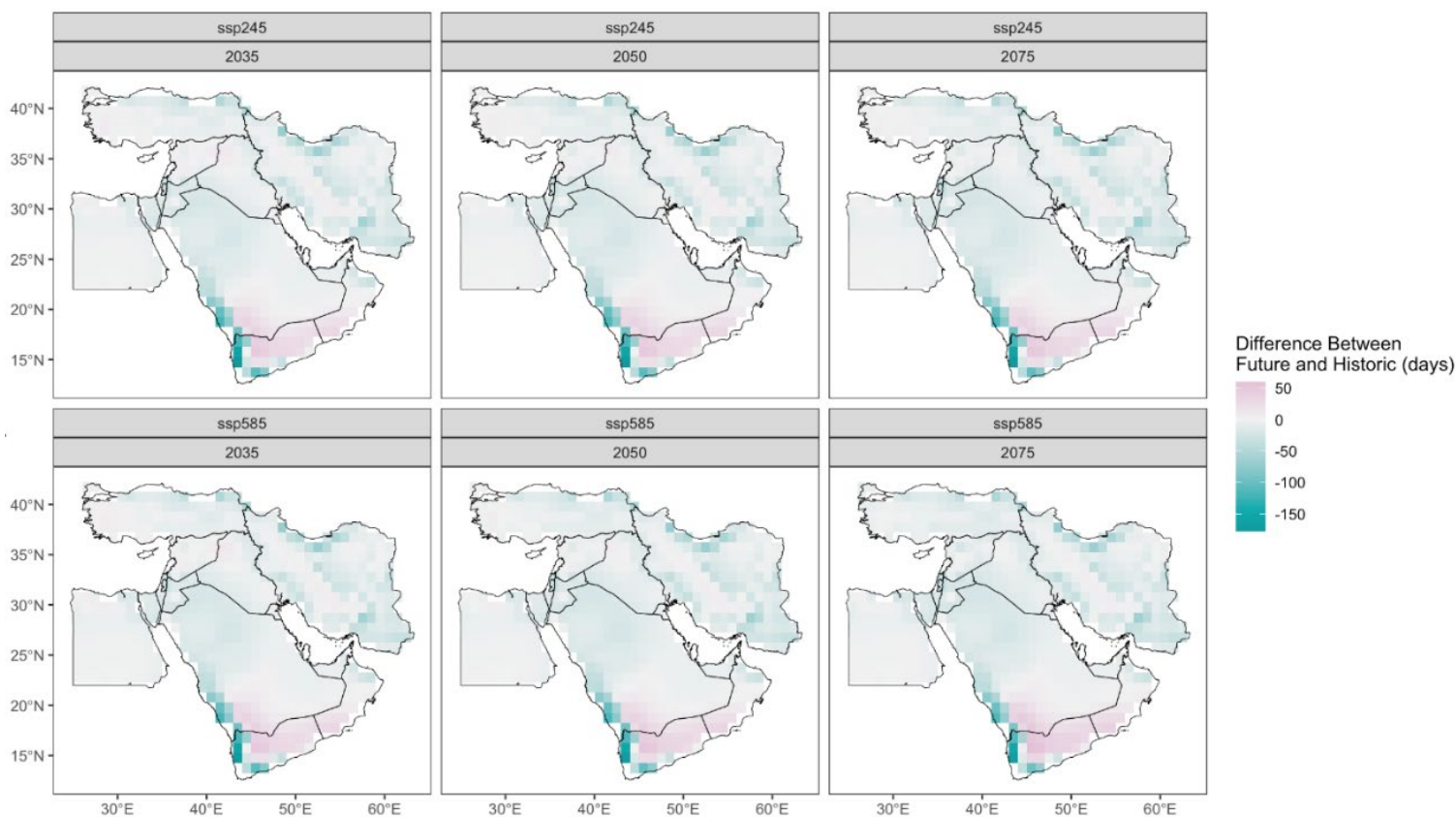
Storms and Coastal Issues

Heavy Precipitation

Flooding from extreme rainfall and cyclones can contaminate freshwater sources with cholera bacteria or other pathogens from untreated sewage. The worst cholera epidemic of modern times has been occurring in Yemen due to the years of conflict, which have severely disrupted water, sanitation, and hygiene (WASH) and healthcare infrastructure; projected flooding could exacerbate the spread of disease. Similarly, WASH infrastructure in Iraq and Syria has been hobbled from war, making these countries particularly vulnerable. Flash floods in Iraq (Nov 2015) caused a regional cholera outbreak, and Syria is experiencing an ongoing outbreak.

Spatial view of future heavy rain days in comparison to historic: 90th percentile historic (1990-2020) rain events were used to define heavy rain days. More heavy localized rainfall events are projected in some regions, such as Yemen, southwest Saudi Arabia, and western Oman. In general, the Intergovernmental Panel on Climate Change (IPCC) Assessment Report 6 (AR6) projects an increase of heavy precipitation and related flooding across the region (medium confidence). Though a decrease is being shown in many areas in Figure 2, an elevated risk remains of rain-based flooding because of other climate factors (i.e., the climate is getting dryer and hotter, which makes the sediment less permeable). When rain falls on impervious soils, the rain moves off faster, similar to a parking lot, so flood risk becomes high. In these model projections little difference exists among the various future scenarios.

Figure 2: Absolute difference between climate projections and historic data for frequency of rain days in the historic 90th percentile



Sea-Level Rise

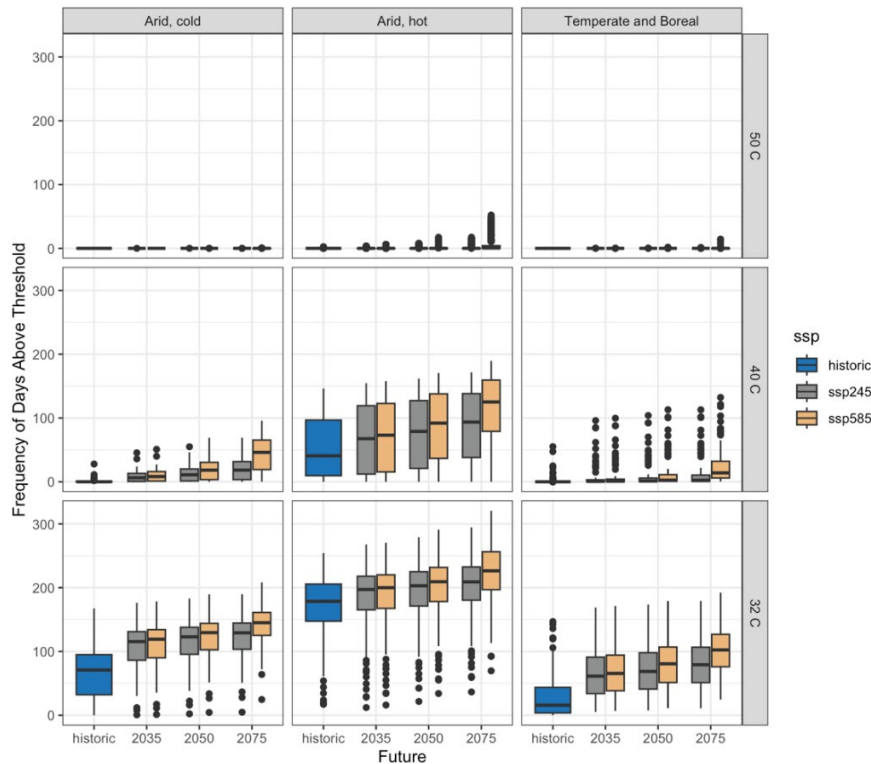
- IPCC Global mean sea level (GMSL) projections:
 - By 2050, RCP 2.6: 0.24 m (0.17–0.32 m, likely range), RCP 8.5: 0.32 m (0.23–0.40 m, likely range) medium confidence.
 - By 2100, RCP 2.6: 0.43 m (0.29–0.59 m, likely range), RCP 8.5: 0.84 m (0.61–1.10 m, likely range).
- GMSL has risen 3.6mm/yr from 2005-2015 (IPCC); 2000-2015 Red Sea rising 6.4mm/yr; Arabian Sea 4.57 mm/yr (Abdulla & Al-Subhi, 2021). More research is needed to better project sea level rise in large, shallow seas.

Extreme Heat

Frequency of Black Flag Days and Higher Temperatures

Figure 3 displays the frequency of days above three different extreme heat thresholds by climate region and different warming scenario. The figure shows that the frequency of days over 32°C and 40°C are projected to increase in all climate zones, but the increase is most drastic in the “Arid, cold” and “Temperate and Boreal” zones. The historical data indicates that days over 50°C did not occur or were very rare in all climate zones. The future projections indicate that all zones will rarely experience these very hot days.

Figure 3: Average number of days per year that three temperature thresholds (50°C, 40°C and 32°C) were reached or exceeded in historic record (1990-2020) and in future climate projections. Each column is a Koppen climate region. Each row is a temperature threshold.



Box Plots – The upper and lower bounds of the colored boxes indicate the upper and lower quartiles of the data. The black horizontal line within the boxes is the median value. The vertical lines pointing up and down away from the colored box indicate the upper and lower extremes of the data. Points beyond these lines are outliers. For a general assessment of the data, one can focus on the colored boxes and the black horizontal median line within each box.

Drought

Figure 4 displays the average annual precipitation by climate region and different warming scenario. From this figure we gather that temperate and boreal regions will be the most impacted by decreases in rainfall. There are outlier years and places that are wet, that will continue to be wet, but these are not the majority.

Figure 4: Average Mean Annual Precipitation

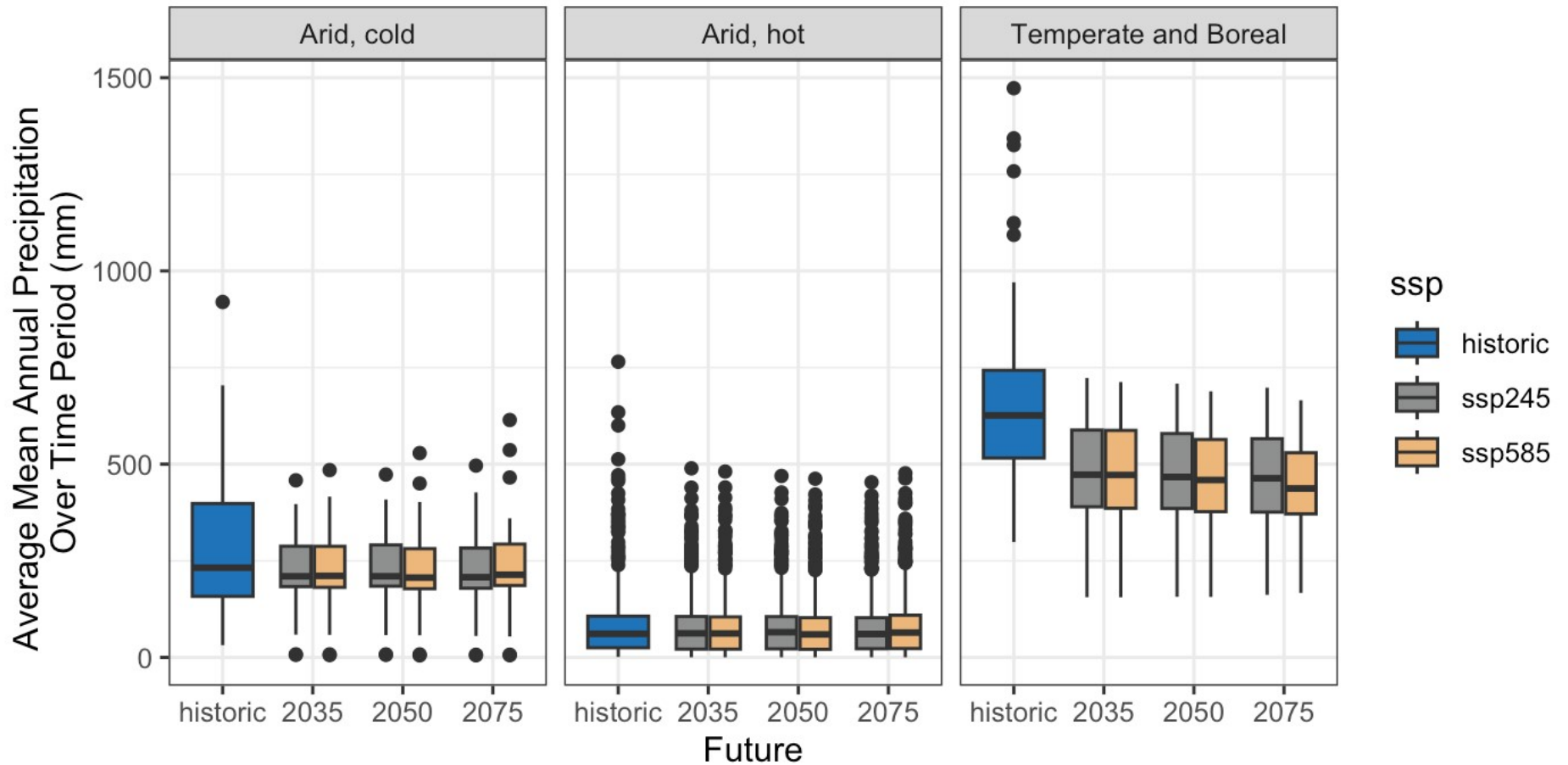


Figure 5 displays the mean maximum number of consecutive dry days to further explore drought by climate region and different warming scenario. From this figure we can see the drought pattern is the same as shown in the map on the Water Supply & Drought slide for each future scenario.

Figure 5: Mean Maximum Number of Consecutive Dry Days

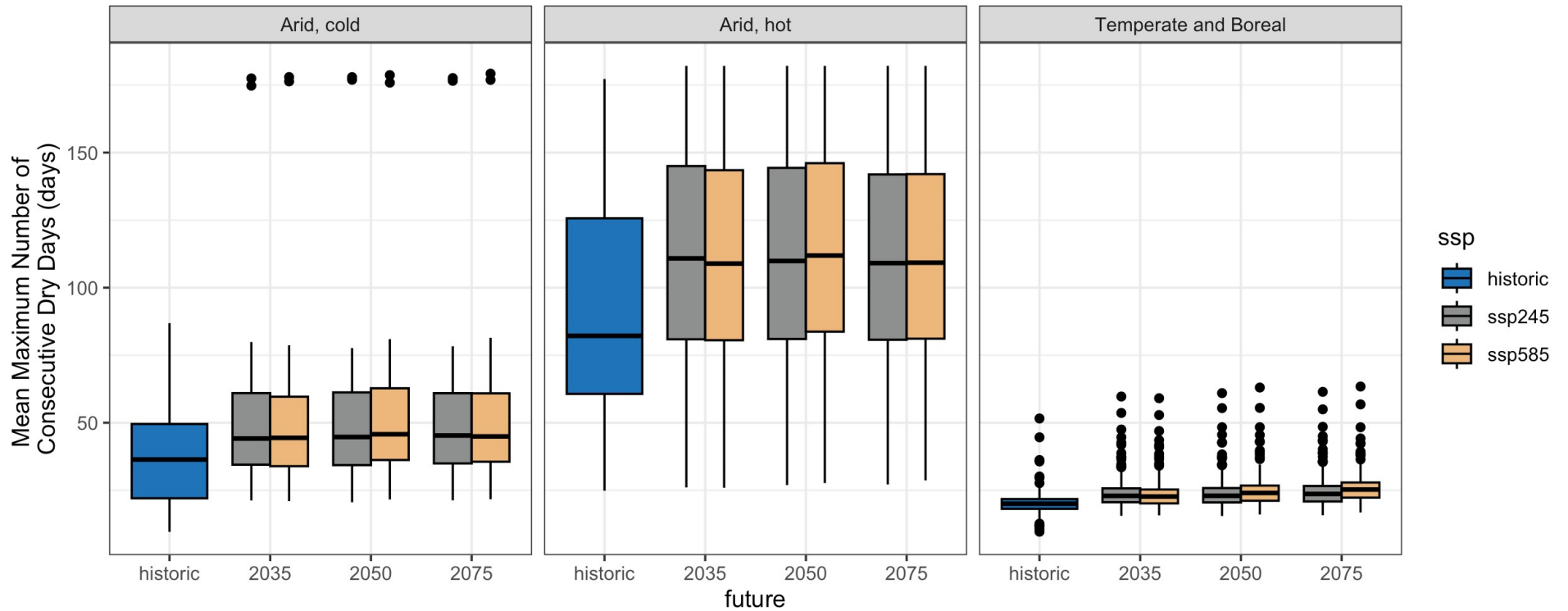
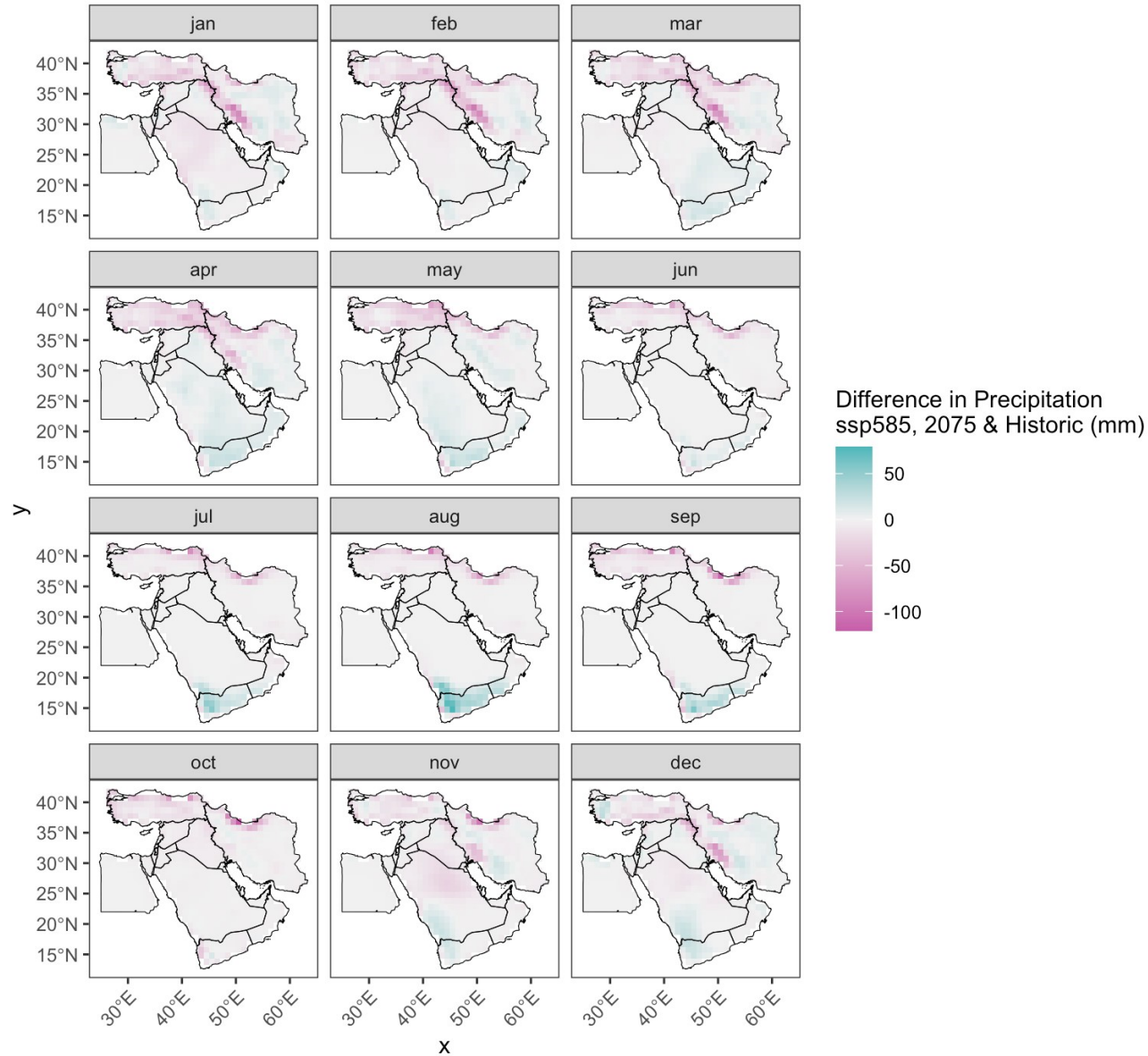


Figure 6 displays the difference in mean precipitation by month between 2075 extreme warming scenario and the historic period. Türkiye and Iran will see less precipitation throughout most of the year.

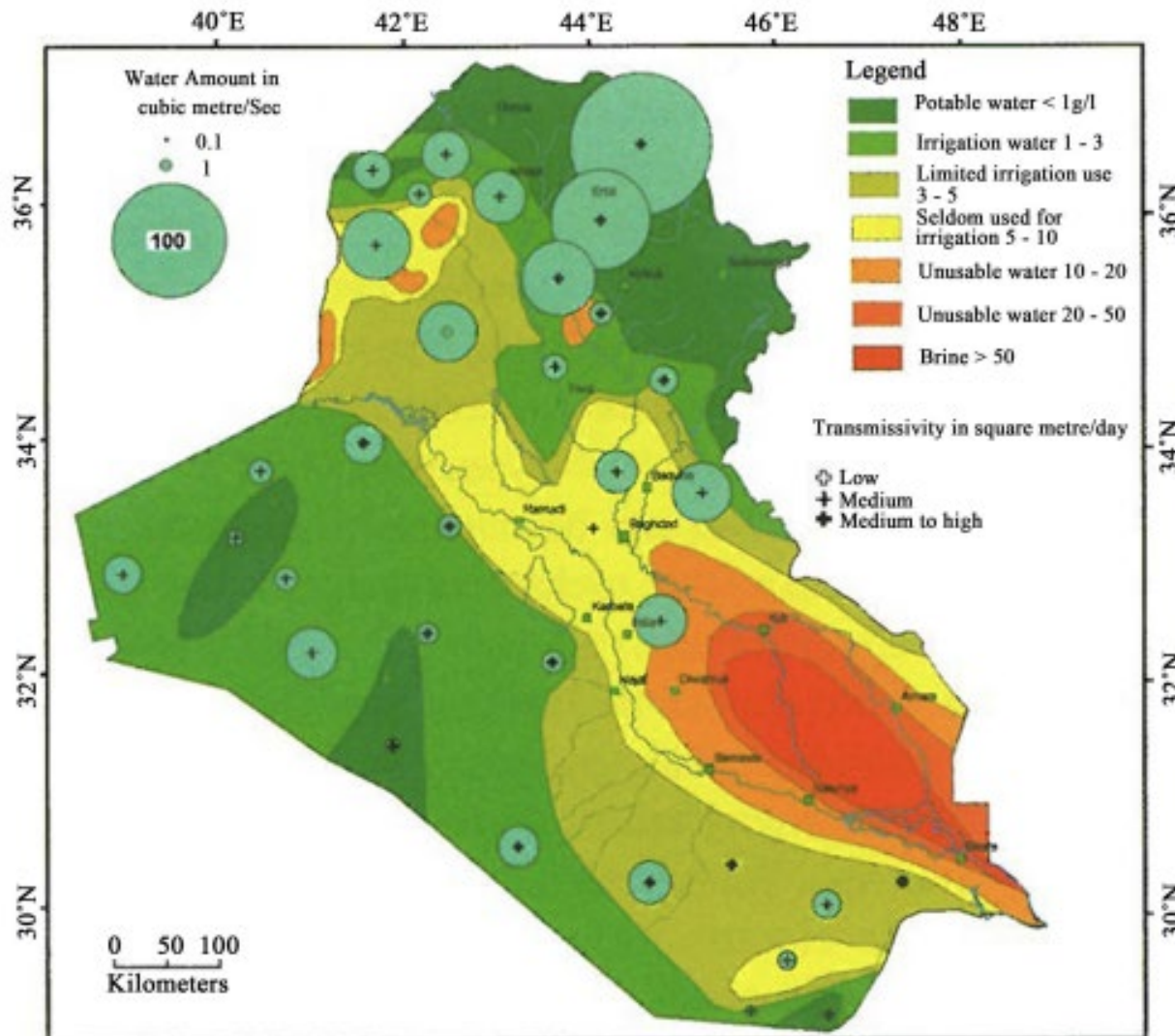
Figure 6: Difference in mean monthly precipitation between 2075 extreme warming scenario, and historic.



Water Supply

Saltwater intrusion in Iraq: Low flows in the Tigris and Euphrates Rivers are increasing the saltwater intrusion into the rivers and groundwater from the Gulf. Figure 7 shows the landward extent to which the intrusion is reaching. This figure complements the *Water Supply and Drought* slide, Key Water Supply Issues noted for the Tigris and Euphrates River systems.

Figure 7: Salinity zones in groundwater; water quantified in cubic meters per second. Image sourced from Figure 7 in Al-Ansari, Nadhir, Ammar A. Ali, and Sven Knutsson. "Present Conditions and Future Challenges of Water Resources Problems in Iraq." *Journal of Water Resource and Protection* 06, no. 12 (2014): 1066–98. <https://doi.org/10.4236/jwrp.2014.612102>.



Climate Change in the Middle East

Figure 8: Map of surface and groundwater for the Middle East, data source: Bundesanstalt für Geowissenschaften und Rohstoffe (BGR) & UNESCO (2008): Groundwater Resources of the World 1 : 25 000 000 – Hannover, Paris. WHYMAP GWR © BGR & UNESCO 2015

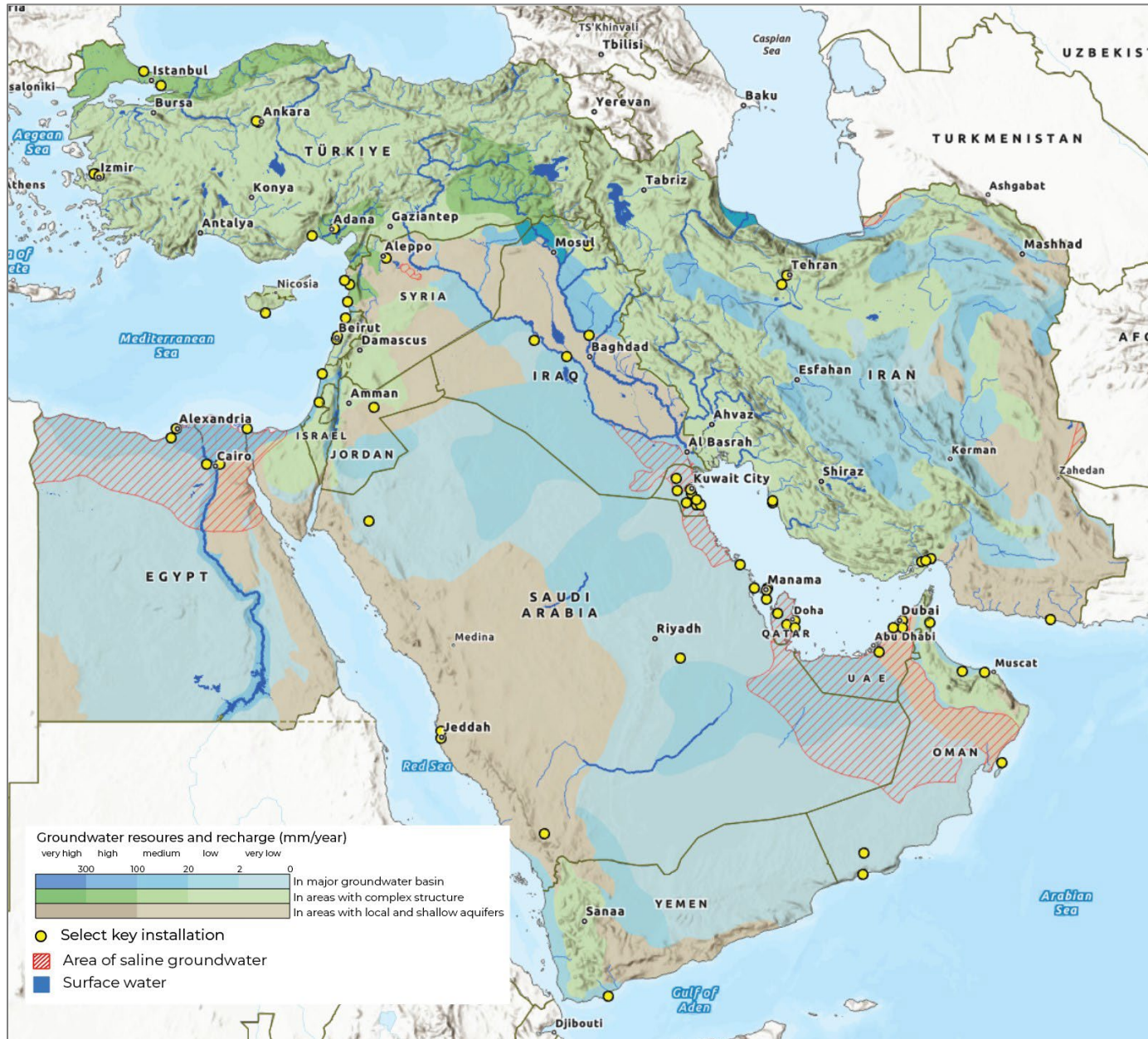
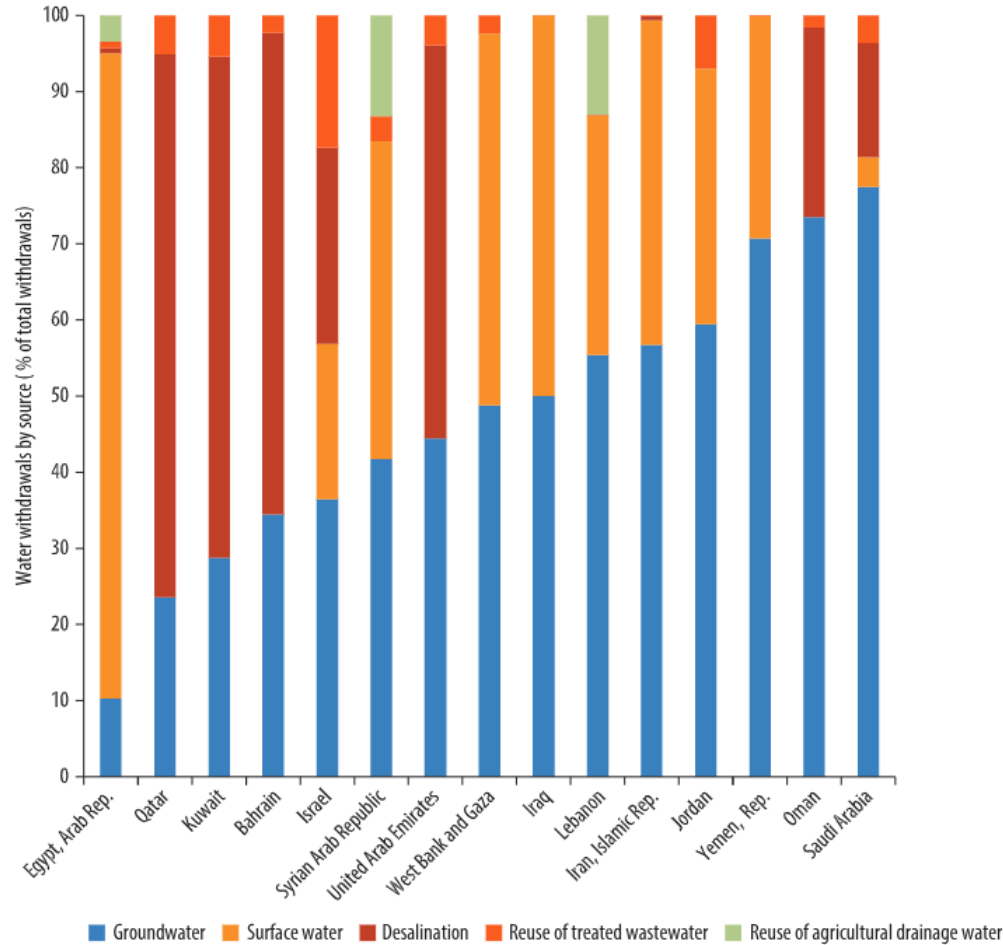


Figure 9: Water withdrawals, by source, as a percentage of total withdrawals, by country and economy, 2010. Image sourced from Figure 2.8 on page 50 in World Bank, 2017. *Beyond Scarcity: Water Security in the Middle East and North Africa*. MENA Development Series. World Bank, Washington, DC. License: Creative Commons Attribution CC BY 3.0 IGO

Water Withdrawals, by Source, as a Percentage of Total Withdrawals, by Country and Economy, 2010



Sources: World Bank calculations. Data on desalination capacity come from Global Water Intelligence 2016a. Data on all other categories are from FAO AQUASTAT.

Note: For Iraq, the Syrian Arab Republic, and West Bank and Gaza, the breakdown between surface and groundwater withdrawals was not available and withdrawals were split equally between the two categories. In absolute terms, the Arab Republic of Egypt has the largest volume of reused of agricultural drainage water, and Saudi Arabia the largest desalination capacity in the region. Caution should be used in comparing data on annual freshwater withdrawals, which are subject to variations in collection and estimation methods.

Wind

Mid-century projections include a decrease in mean wind speed over the Mediterranean (high confidence), but an overall increase in severe windstorms (medium confidence). There is low confidence in wind projections for the Arabian Peninsula. (Arias et al. 2019)

High winds can cause shipping issues in marginal seas. Suez Canal was blocked by cargo ship for 6 days in March 2021 from high winds wedging the ship into the canal banks.

Given the projected increases in temperatures and reduced precipitation, any increases in wind could drive in increase in devastating sand and dust storms.

Data Analysis Methods

Historical Data

- Historical data were from the 5th generation European Centre for Medium-Range Weather Forecasts atmospheric reanalysis (ERA5) data. These data were accessed through Google Earth Engine. Historic data refer to the time range between January 1, 1990, and June 30, 2020, and are averaged over this time period. These data are referred to 'historic' throughout the analysis.
- We used daily and monthly precipitation totals, maximum daily temperature, and monthly average temperature.

Future Climate Projections

- Climate projections were from the 6th phase of the Coupled Model Intercomparison Project (CMIP6). These data were accessed through NASA Earth Exchange which downscales and bias corrects CMIP6 models.
- We used climate projections over two climate change scenarios (SSP 245 and SSP 585) and for three future timeframes (2035, 2050, 2075). Each future timeframe is taken as the average values of the 20 years surrounding the target year: 2035 is the average of 2026 to 2045, 2050 is the average of 2041 to 2060, 2075 is the average of 2066 to 2085.
- We used data from 18 different models for future projections (ACCESS-ESM1-5, BCC-CSM2-MR, CanESM5, CMCC-ESM2, CNRM-ESM2-1, EC-Earth3-Veg-LR, FGOALS-g3, GFDL-ESM4, GISS-E2-1-G, INM-CM5-0, IPSL-CM6A-LR, KIOST-ESM MIROC-ES2L, MPI-ESM1-2-HR, MRI-ESM2-0, NESM3, NorESM2-MM, TaiESM1). The TaiESM1 model was not included for temperature analyses because it tends to predict much warmer futures than the other models.
- All future data are averaged over the 18 models and over the 20 years surrounding the target future year.
- We pulled daily data for precipitation rates (which was converted to total daily precipitation), maximum daily temperature, and mean daily temperature.

Metrics

All metrics were calculated for both historical data and future climate projections.

- Heavy Rain Days
 - o Heavy rain days were calculated as the top 90th percentile of rain events from the historic data within the three Koppen regions (2.36 mm, 0.23 mm, and 5.76 mm thresholds for arid cold, arid hot, and temperate & boreal regions, respectively).
 - o The frequency of these heavy rain days was calculated for each raster cell over for the two future SSP and averaged for a yearly average within a future scenario.

- Mean Annual Precipitation
 - o The total precipitation for year, averaged over the given time period.
- Temperature Thresholds
 - o For each temperature threshold (32°C, 40°C, and 50°C), the frequency of days within a year that the maximum temperature reached or exceeded the threshold were quantified.
- Mean Monthly Temperature
 - o Mean monthly temperatures were calculated for historic and future climate projections.
- Density Altitude
 - o Density altitude was calculated using the equations:

$$PA = (P_0 - P_{AltSet}) * 1000 + H_{airport}$$

$$DA = PA + 120 * ([T_0 - 0.002H_{airport}] - T_s)$$

Where PA is pressure altitude, P_0 is the standard pressure (29.92 in Hg), P_{AltSet} is the altimeter setting in in Hg, $H_{airport}$ is the elevation in feet, DA is the density altitude in feet, T_0 is the standard temperature at sea level (15 C), and T_s the observed air temperature in C.

- o For future projections, we held PAltSet at 29.95 in Hg for our calculations of density altitude over the set of future temperature projections. Air temperature was the mean temperature between June and August from historical and projected future data. Elevation data were from the ASTER DEM data set (<https://asterweb.jpl.nasa.gov/gdem.asp>).
- Consecutive Dry Days
 - o Consecutive dry days were defined as a 24-hour period with less than 1mm of rainfall (<https://www.int-res.com/articles/cr2002/19/c019p193.pdf>). We calculated the maximum consecutive dry days (e.g., the longest time period with no rain) within a year for each raster cell. This maximum was then averaged over the historical or future period.